

**Non-Markovian collisional dynamics probed with laser-aligned molecules**M. Bournazel<sup>1</sup>, J. Ma<sup>1,2</sup>, F. Billard<sup>1</sup>, E. Hertz<sup>1</sup>, J. Wu<sup>2</sup>, C. Boulet<sup>3</sup>, J.-M. Hartmann<sup>4,\*</sup> and O. Faucher<sup>1,†</sup><sup>1</sup>*Laboratoire Interdisciplinaire CARNOT de Bourgogne, UMR 6303, Centre National de la Recherche Scientifique, Université de Bourgogne, BP 47870, 21078 Dijon, France*<sup>2</sup>*State Key Laboratory of Precision Spectroscopy, East China Normal University, Shanghai 200241, China and Collaborative Innovation Center of Extreme Optics, Shanxi University, Taiyuan, Shanxi 030006, China*<sup>3</sup>*Institut des Sciences Moléculaires d'Orsay, Centre National de la Recherche Scientifique, Université Paris-Saclay, F-91405 Orsay, France*<sup>4</sup>*Laboratoire de Météorologie Dynamique, IPSL, Centre National de la Recherche Scientifique, École Polytechnique, Institut Polytechnique de Paris, Sorbonne Université, École Normale Supérieure, Université PSL, F-91120 Palaiseau, France*

(Received 29 August 2022; accepted 8 February 2023; published 24 February 2023)

The Markov, as well as the secular, approximations are key assumptions that have been widely used to model decoherence in a large variety of open quantum systems, but, as far as intermolecular collisions are considered, very little has been done in the time domain. In order to probe the limits of both approximations, we here study the influence of pressure on the alignment revivals (echoes) created in properly chosen gas mixtures (HCl and CO<sub>2</sub>, pure and diluted in He) by one (two) intense and short laser pulse(s). Experiments and direct predictions using molecular-dynamics simulations consistently demonstrate, through analyses at very short times (<15 ps) after the laser kick(s), the breakdown of these approximations in some of the selected systems. We show that the nonadiabatic laser-induced molecular alignment technique and model used in this paper directly provide detailed information on the physical mechanisms involved in the collisional dissipation. Besides this “fundamental” interest, our findings also have potential practical applications for radiative heat transfer in planetary atmospheres and climate studies. Indeed, short time delays in the dipole autocorrelation function monitoring the light absorption spectrum correspond to large detunings from the optical resonances in the frequency domain, thus influencing the atmospheric transparency windows. Furthermore, the fact that the approach tested here for linear rotors can potentially be applied to almost any gas mixture (including, for instance, nonlinear and/or reacting molecules) further strengthens and broadens the perspectives that it opens.

DOI: [10.1103/PhysRevA.107.023115](https://doi.org/10.1103/PhysRevA.107.023115)**I. INTRODUCTION**

All open quantum systems in contact with an un-controlled environment (the bath) are subject to dissipation effects. The fact that this occurs in most natural phenomena has stimulated researches in diverse scientific fields in order to understand the processes at play. Within this frame, modeling the effect of dissipation on quantum coherences is a key issue. However, since this generally involves very challenging (formal, computational, and of needed input data availability) difficulties, most theoretical studies have used the so-called secular and/or Markov approximations. The first neglects environment-induced transfers between coherences of different frequencies as well as those between coherences and populations, which enables one to disregard all the associated terms in the master equation driving the system evolution through its density matrix. The second considers that all events (e.g., collisions) leading to a given process (e.g., decoherence, energy transfer, and pressure broadening of light-absorption, -emission, and -scattering spectra) are complete and uncorrelated. There are then no memory effects

in the system-bath “history” which is thus assumed to be a Markov chain of instantaneous and independent events. Since these approximations have been investigated or used in a plethora of studies, as made obvious by a quick bibliography search, a literature review on this issue is beyond the scope of this paper, but the interested reader is invited to consult Refs. [1–4]. Nevertheless, note that a broad range of phenomena and applications is involved, with far from exhaustive examples given by quantum heat engines [5], quantum information and computing [6], human vision [7], light-harvesting complexes [8], light absorption and scattering [9], and transports of mass and energy [10,11].

As far as non-Markovianity and nonsecularity in collision-induced rotational relaxation and decoherence in gas media (on which this paper focuses) are concerned, practically nothing has been done in the time domain. Indeed, to the best of our knowledge, it is only recently that nonsecular effects have been pointed out in a study of N<sub>2</sub>O-He gas mixtures (which is a Markovian system) [12]. The present paper thus fills a scientific gap by investigating, in the time domain, the limits of the Markov approximation for collision-induced rotational decoherence in molecular gases.

Recall that nonsecularity and non-Markovianity in intermolecular collisions are commonly denoted [9,13] in frequency-domain studies of light-matter interaction spectra

\*jean-michel.hartmann@lmd.ipsl.fr

†olivier.faucher@u-bourgogne.fr

TABLE I. Expected characteristics of the pressure-induced dynamics in systems probed at the very first instants (typically,  $t < 15$  ps) of decoherence.

	Markovian	Non Markovian
Secular	HCl-He	HCl-HCl
Nonsecular	CO <sub>2</sub> -He	CO <sub>2</sub> -CO <sub>2</sub>

as “line-mixing” and “finite-duration-of-collision” effects, respectively. The former, neglected by the secular approximation, result in transfers of intensity from the weak to the strong absorption region of the spectrum (see Chap. IV of [9] and references therein), which is the frequency-domain counterpart of the fact that the secular approximation overestimates the decoherence rate at the early stage of the relaxation process, as shown below and in [12]. Since disregarding the role of incomplete collisions corresponds to assuming instantaneous intermolecular interactions, the Markov approximation is often denoted in frequency-domain spectroscopic studies as “impact” (or “sudden”). As we show in this paper, the non-Markovian nature of collisions increases the decoherence rate at short times, which manifests itself in the spectral domain by an increase of the absorption of light in the wings of the lines and bands, as shown for CO<sub>2</sub> in [14] and for HCl in [15].

To test the limit of the Markov (and secular) approximation in the time domain, we study the decay of the molecular-axis alignment [16] soon after excitation by short and intense laser pulse(s). Four systems listed in Table I have been retained, which involve, at the investigated time scale, all situations: practically secular and Markovian (HCl diluted in He) or non-Markovian (pure HCl), nonsecular and Markovian (CO<sub>2</sub> diluted in He), or non-Markovian (pure CO<sub>2</sub>).

The remainder of this paper is divided into five sections. We first use simple considerations about the secular and Markov approximations to explain how and why the above-mentioned systems were chosen (Sec. II), before presenting the experiments (Sec. III) and the model used (Sec. IV). The measured and predicted results for the time dependence of the collision-induced decoherence for the four retained systems, probed through molecular alignment, are then presented and discussed in Sec. V. Finally, the respective interests of time- and frequency-domain investigations to probe the limits of the secular and Markov approximations are discussed in Sec. VI, before concluding remarks (Sec. VII).

## II. CHOOSING THE MOLECULAR SYSTEMS

In order to explain how and why we chose the molecular systems retained in this paper, we below recall which parameters condition the validity of the secular and Markovian approximations for the collisional relaxation and associated effects on the molecular rotational alignment.

### A. Secularity

As is well known [16–20], a short and intense laser pulse generates rotational coherences in molecular gases through the creation of nonzero off-diagonal elements in the density matrix  $\rho(t)$ . Under collision-free conditions, these

elements oscillate at frequencies given by the difference between the energies of the coupled rotational states. The postpulse evolution of a coherence  $|J'M'\rangle\langle JM|$ , for a linear molecule, neglecting centrifugal distortion, is then driven by  $\exp(i\omega_{J',J}t) = \exp[i(E_{J'} - E_J)t/\hbar] = \exp\{iB[J'(J'+1) - J(J+1)]t/\hbar\}$ , where  $J$  and  $M$  are rotational and magnetic quantum numbers and  $B$  is the rotational constant. In the presence of collisions, exchanges between coherences associated with different  $(J, J')$  couples occur, but they can be neglected for long enough time delays after the laser excitation, when their relative dephasing (or beating),  $|\omega_{J',J_2} - \omega_{J',J_1}|t$ , is greater than a few times  $\pi$ , according to  $|\text{sinc}(\omega_{J',J_2} - \omega_{J',J_1})t| \ll 1$  [12]. A criterion for neglecting all exchanges between the  $|J_2\rangle\langle J_2| \neq |J_1\rangle\langle J_1|$  coherences, which is precisely the secular approximation, can be derived by considering the “closest” coherences and the fact that a nonresonant laser pulse implies  $J' = J \pm 2$ . One can choose, for instance,  $J'_1 = J_1 + 2$ ,  $J'_2 = J_2 + 2$ , and  $J_2 = J_1 + \Delta J$ , with  $\Delta J = 1$  or  $2$  according to the existence, for the considered molecule, of all (HCl case) or only even (CO<sub>2</sub> case)  $J$  values. This leads to a dephasing of  $|\omega_{J',J_2} - \omega_{J',J_1}|t = 4\Delta JBt/\hbar$  for which the above-mentioned sinc function has reduced to 0.05 for  $4\Delta JBt/\hbar \geq 6\pi$ , i.e.,  $t \geq t_0 = 3h/(4\Delta JB)$  (recall that this criterion is conservative since it is obtained from the dephasing between density-matrix elements and does not depend on the efficiency of collisions). This led us to the choices of CO<sub>2</sub> ( $B = 0.39$  cm<sup>-1</sup>,  $\Delta J = 2$ ), as a prototype nonsecular molecule since its behavior is secular only after  $t_0 \approx 30$  ps, and of HCl ( $B = 10$  cm<sup>-1</sup>,  $\Delta J = 1$ ) as a secular prototype since nonsecular effects only extend up to  $t_0 \approx 2.5$  ps, both values of  $t_0$  being confirmed by Fig. 1.

### B. Markovianity

The Markov approximation here consists in neglecting the fact that some molecules are experiencing a collision when the system is excited. Indeed, their later behavior carries the memory of their prior interactions with the bath. Criteria for Markovianity must thus consider both the relative number of molecules which are significantly interacting with another at a given time and the duration over which this interaction lasts.

We here present details about the choice of pure CO<sub>2</sub> and HCl as prototype non-Markovian systems and CO<sub>2</sub>-He and HCl-He as Markovian ones. For this, we first carried molecular-dynamics simulations, as explained in Sec. IV, for pure CO<sub>2</sub> and CO<sub>2</sub> diluted in He under thermodynamic equilibrium conditions. We extracted from them the relative number of molecules  $N_J(t)$  which are in the rotational level  $J$  at  $t = 0$  and are still there with an unchanged rotational energy at time  $t > 0$ . The results obtained at room temperature for several  $J$  values are plotted in Figs. 2(a) and 2(b). As can be seen, the decay of  $N_J(t)$  is well represented by an exponential law for CO<sub>2</sub> in He over the entire range of the plot, even at very early times, while it is not the case for pure CO<sub>2</sub> which shows a quicker decay at short times than at longer ones. Note that extrapolating the long-time exponential to  $t=0$  points out the “initial slip” effect [21], a characteristic signature of non-Markovian dynamics. These results, which indicate that the Markov model is suitable for interactions of CO<sub>2</sub> with He but not for those with CO<sub>2</sub>, result from the influence of

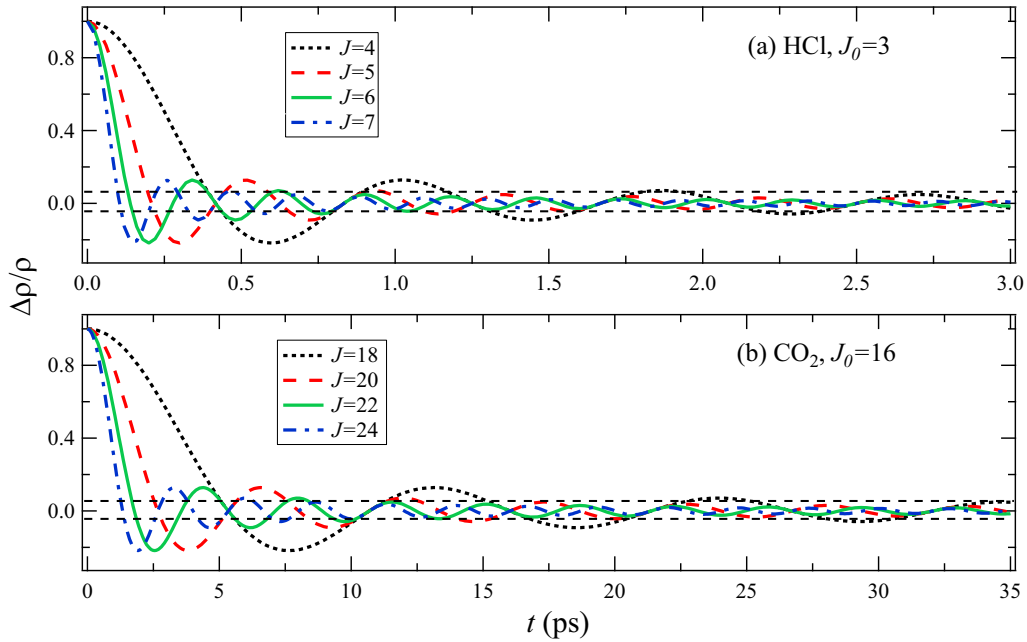


FIG. 1. Relative modification of the  $|J_0 M_0\rangle$  ( $J_0 + 2M_0$ ) coherence induced by collisional transfers from the coherences  $|JM\rangle \langle J + 2M|$  (all normalized to unity at  $t = 0$ ) in the cases of HCl (a) and CO<sub>2</sub> (b) for the most populated level at room temperature ( $J_0 = 3$  and 16, respectively). The dashed lines indicate the  $\pm 5\%$  levels. See the Supplementary Information (Note 2) in [12] for details on the computational procedure used.

the incomplete collisions associated to those molecules which are already significantly interacting with a partner at  $t = 0$ . The difference between the behaviors of CO<sub>2</sub> in He and pure CO<sub>2</sub> (similar results being predicted for HCl-He and pure HCl, respectively) can be explained, as done below, by the relative translational speeds of the collision partners and the characteristics of the intermolecular potential-energy surfaces (PESs) involved.

For CO<sub>2</sub>-He, the PES has an almost negligible well (with respect to the kinetic temperature at 295 K) and a repulsive front whose relevant part lies within the 3.5- to 4.0-Å range of the C-He distance (see Fig. 1 of [22]). This implies that, for a CO<sub>2</sub> molecule to be colliding with an He atom at  $t = 0$ , the latter should be located in the interval between the two spheres centered on the C atom and of radii 3.5 to 4.0 Å. This corresponds to a very small volume ( $\simeq 90 \text{ \AA}^3$ ) that statistically contains very few He atoms (for 5 amagat which corresponds to  $1.34 \times 10^{26} \text{ atom/m}^3$ , this statistical number is about 0.01). In addition, the mean relative speed of CO<sub>2</sub>-He collisions at 295 K is 1300 m/s, which means that the distance between the two spheres ( $0.5 \text{ \AA}$ ) is, on average, traveled in 38 fs. The above given numbers show that non-Markovian effects are very small and only exist at times scales much shorter than those investigated in this paper.

For pure CO<sub>2</sub>, the situation is very different due to both the significantly slower relative speed of collisions and the much broader range of distances within which intermolecular forces are large. Indeed, the CO<sub>2</sub>-CO<sub>2</sub> intermolecular potential has a repulsive front around 3 Å and is significant for C-C distances up to 6 Å (see Fig. 3 in [23]). In this case, the volume ( $\simeq 800 \text{ \AA}^3$ ) between the two spheres where a collision partner should be at time  $t = 0$  and the statistical number ( $\simeq 0.1$  at 5 amagat) of particles within this volume are ten times larger than for He. In addition, the difference

of the radii of these spheres ( $3 \text{ \AA}$ ) is traveled, for the pure CO<sub>2</sub> mean relative speed of 530 m/s, in about 0.5 ps [in agreement with the time interval where the population decay in Fig. 2(b) is much faster than at long delays]. It is thus obvious that non-Markovian effects impact the behavior of pure CO<sub>2</sub> at the early stage of the collision-induced rotational relaxation and decoherence processes, contrary to the case of CO<sub>2</sub> interacting with He. It should be pointed out that the fact that the pure CO<sub>2</sub> results in Fig. 2 deviate from a purely exponential behavior only before about 0.5 ps does not imply that the Markov approximation is valid right after this time. Indeed, a Markovian behavior is only obtained once the apparent density-normalized decay time constant  $\tau_J(t)$ , such that  $N_J(t)/N_J(t=0) = \exp[-t/\tau_J(t)]$ , becomes independent of  $t$ . From the results in Fig. 2(a), one can show that this plateau is reached only around 20 ps. For CO<sub>2</sub>-CO<sub>2</sub> collisions, non-Markovian effects will thus significantly influence the decay with pressure of the alignment echo amplitude up to  $\tau_{12} \approx 10$  ps, as confirmed by the results presented in Sec. V. Finally, note that the facts that the decays in Figs. 2(a) and 2(b) increase with  $J$  for pure CO<sub>2</sub>, while they are almost  $J$  independent for CO<sub>2</sub> colliding with He, result from the large difference in the duration of efficient collisions between CO<sub>2</sub>-CO<sub>2</sub> and CO<sub>2</sub>-He pairs.

### III. EXPERIMENT

The experimental study of the aforementioned systems has been performed through two different configurations. To probe the short-time collisional relaxation of CO<sub>2</sub>, it was necessary, due to its long rotational period (42.7 ps), to align the molecules using two pump pulses (denoted below as  $P_1$  and  $P_2$ ) delayed by  $\tau_{12}$ , leading to the formation of a rotational echo [24–26] at  $2\tau_{12}$ , whereas the rotational period of HCl

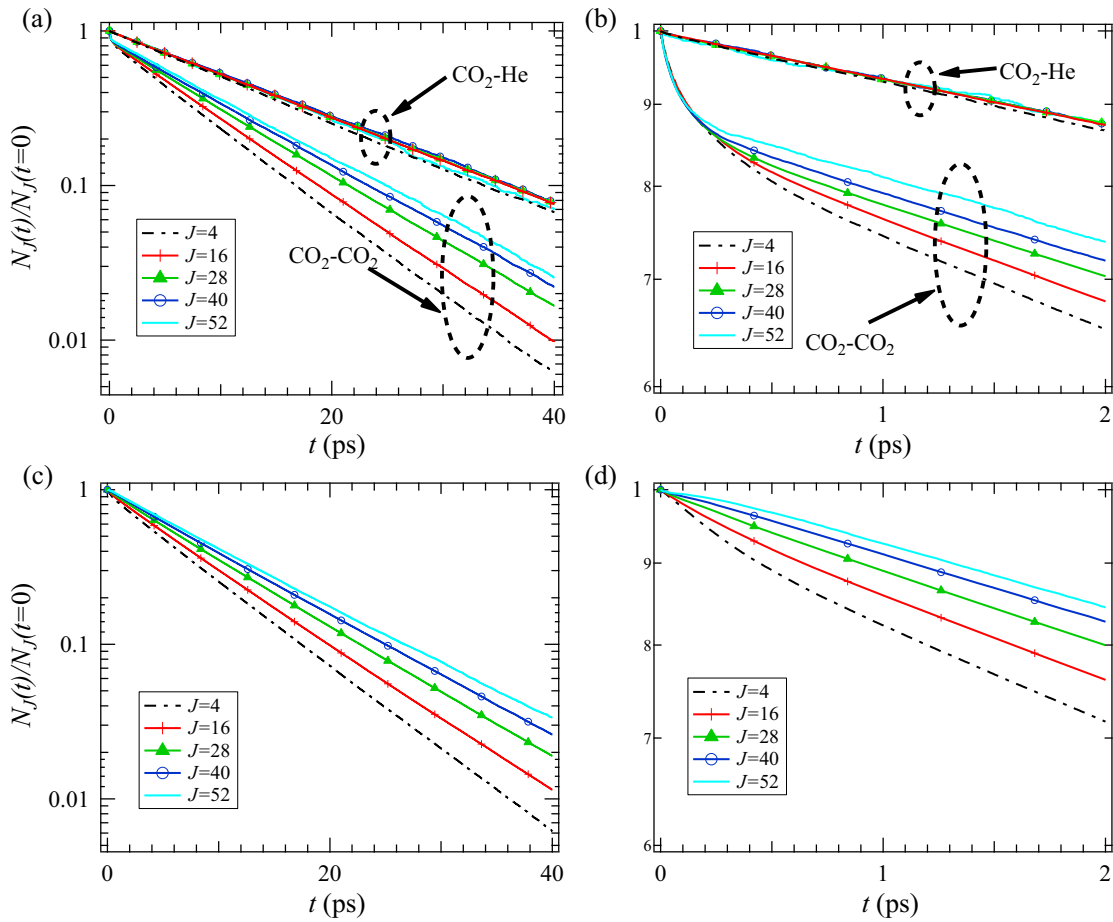


FIG. 2. (a) Computed relative evolution with time of the number of CO<sub>2</sub> molecules in the rotational  $J$  state at time  $t = 0$  which are still in this level at time  $t > 0$  for pure CO<sub>2</sub> and CO<sub>2</sub> infinitely diluted in He and a gas density  $d$  of 5 amagat (1 amagat is the number of molecules of an ideal gas per unit volume at STP). (b) Same results plotted in a reduced time range, with a zoom on short times. (c), (d) Same as (a) and (b) but here only for pure CO<sub>2</sub> and obtained under the Markovian approximation, after removal of all the molecules which are significantly interacting with another at  $t = 0$ .

(1.50 ps) was short enough to track the dissipation using the alignment revivals induced by a single laser pulse.

The experimental setup is presented in Fig. 3. The laser beam was produced by a chirped-pulse amplified Ti:sapphire laser (not shown) delivering nonresonant pulses centered at

800 nm, of 100-fs duration (full width at half maximum), and operating at 1-kHz repetition rate. A beam splitter was placed at the output of the laser to produce a probe beam, vertically polarized, and a pump beam, polarized at 45° with respect to the probe beam. The latter was frequency doubled in a beta

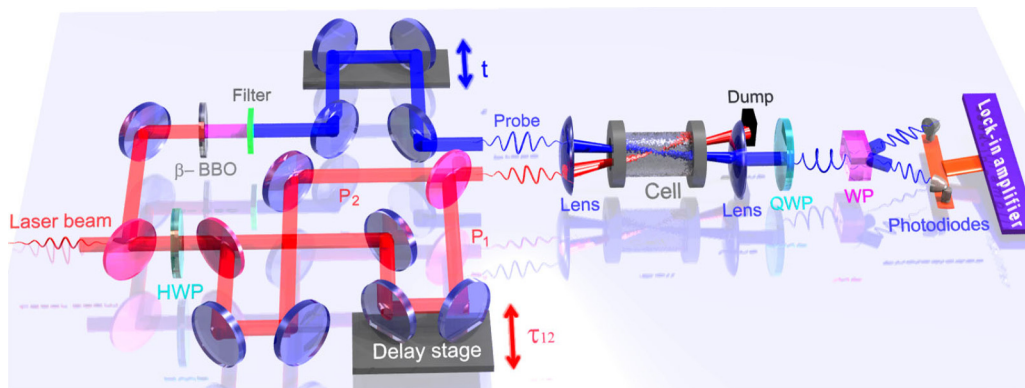


FIG. 3. Experimental pump-probe setup for measuring ultrafast collisional dissipation of rotational coherences by probing either molecular alignment revivals (using a single pump pulse  $P_1$ ) or rotational echoes (using both pump pulses  $P_1$  and  $P_2$ ). HWP, half-wave plate; QWP, quarter-wave plate; WP, Wollaston prism.  $\tau_{12}$  and  $t$  denote the temporal delay between  $P_1$  and  $P_2$  and between  $P_1$  and the probe pulse, respectively.

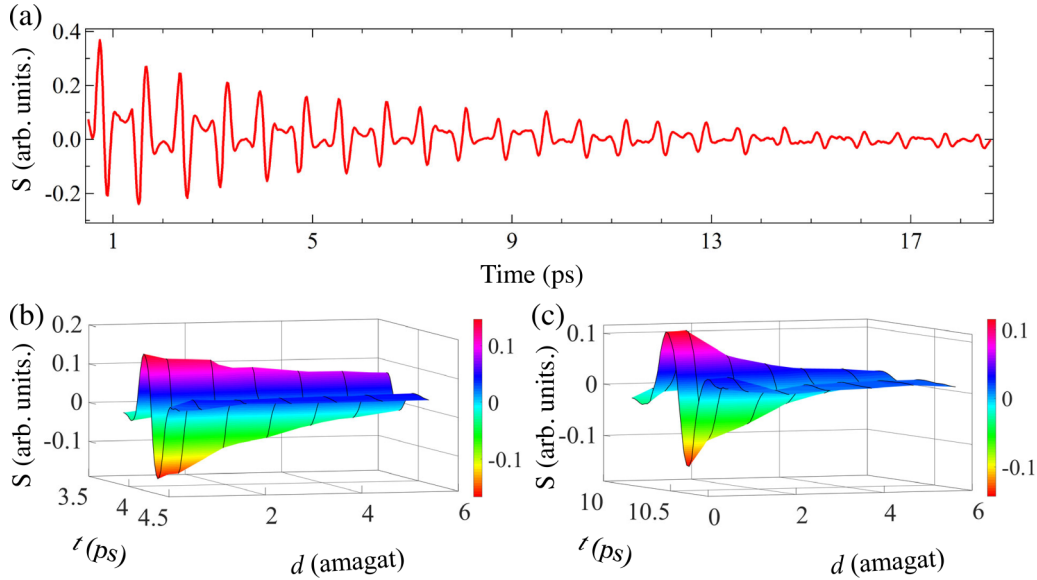


FIG. 4. (a) Alignment trace measured in 3 bars of pure HCl for a laser peak intensity estimated around  $20 \text{ TW/cm}^2$ . Three-dimensional representation of the density-normalized alignment signals measured for different densities  $d$  (1 amagat corresponding to  $2.69 \times 10^{25}$  molecules/ $\text{m}^3$ ) around the (b) 5th and (c) 13th revival at  $t = 4.05$  and  $10.45$  ps, respectively. The black vertical lines on the colored maps in (b) and (c) indicate the densities for which measurements were made. The colorbars represent the amplitude of the signal.

barium borate crystal enabling a filtering out of the 800-nm light scattered by the gas cell on the detectors. The 800- and 400-nm pulses were temporally delayed using a motorized stage equipped with a corner cube reflector. In the case of the two excitation pulses setup, in order to create rotational echoes, a second beam splitter was added to the path of the pump  $P_1$  to create a second pump beam  $P_2$  with the same polarization and same direction of propagation as  $P_1$ , and with an adjustable time delay  $\tau_{12}$  monitored by a second motorized stage placed on the  $P_1$  path. The two pump beams were then focused, using a plano-convex lens, on a high-pressure static cell filled with the gas sample. The optical anisotropy following the alignment of the molecules along the electric field of the pump(s) was measured by a probe pulse with a balanced detection [27] providing a signal proportional to the alignment factor  $\langle \cos^2 \theta - 1/3 \rangle(t)$ , where  $\langle \rangle$  denotes an ensemble average and  $\theta$  is the angle between the molecular axis and the direction of the (linear) polarization of the pump pulse(s).

Echoes of  $\text{CO}_2$ , pure and diluted in 96% He, have been recorded for fixed delays  $\tau_{12}$ , chosen such that the echo at  $2\tau_{12}$  after  $P_1$  appears before the first alignment revival (at  $t = 10.6$  ps), and various total gas pressures from 6 to 18 bars and from 7 to 24 bars, respectively. Similarly, the series of revivals following the excitation of HCl, pure and diluted in 95% He, by a single pulse have also been recorded for pressures ranging from 0.5 bar to 6 bars and from 5 to 40 bars, respectively. All measurements have been made at room temperature for pulse intensities between 20 and  $40 \text{ TW/cm}^2$ . A measured alignment trace of pure HCl is shown in Fig. 4, which, incidentally, constitutes the first realization of laser-induced alignment of this molecule, as well as two of its revivals recorded for different gas densities  $d$ . The density-normalized decay time constant  $\tau_R(t_R)$  (in ps amagat) as a function of the revival time  $t_R$  was obtained by subtracting the permanent component from the alignment trace [17] and

then fitting the peak-to-dip amplitudes  $S(t_R, d)$  of the revivals versus  $d$ , using the expression  $S(t_R, d) \propto \exp[-t_R d / \tau_R(t_R)]$ . The same procedure was applied to  $\text{CO}_2$  in order to extract the decay time constants of the echoes  $\tau_E(2\tau_{12})$  as a function of  $\tau_{12}$ , as done in [12].

#### IV. THEORY

Alignment traces for the considered systems were predicted using classical molecular-dynamics simulations, following the approach detailed in [18,28] briefly recalled below. The molecules (and atoms) are placed inside a cubic box, with periodic boundary conditions [29], of dimensions defined by the chosen number of particles and total gas density. Their positions are chosen randomly with the constraint that they should not be too close to each other in order to avoid nonphysically strong interactions between pairs. The translational velocities were initialized according to the Boltzmann statistics with, for the molecules, random axis orientations and a Boltzmann distribution of the rotational angular momentum vectors. Then the evolution with time of all these parameters is computed using laws of classical mechanics [28]. For this, the torque and force applied to each molecule and atom resulting from its interaction with the neighboring collision partners are computed using the intermolecular potentials from [22,23,30,31] for  $\text{CO}_2$ -He, pure  $\text{CO}_2$ , HCl-He, and pure HCl, respectively. Note that in order to simulate  $\text{CO}_2$  and HCl infinitely diluted in He at a reasonable computational cost, mixtures containing 50% of He were treated while disregarding all molecule-molecule interactions. During the electromagnetic excitation(s) the torque is computed [28] from the laser pulse(s) experimental characteristics using the anisotropic polarizabilities from [32] for HCl and [33] for  $\text{CO}_2$ . Once the time evolution of the axis orientation of each molecule is known, the alignment factor  $\langle \cos^2 \theta -$

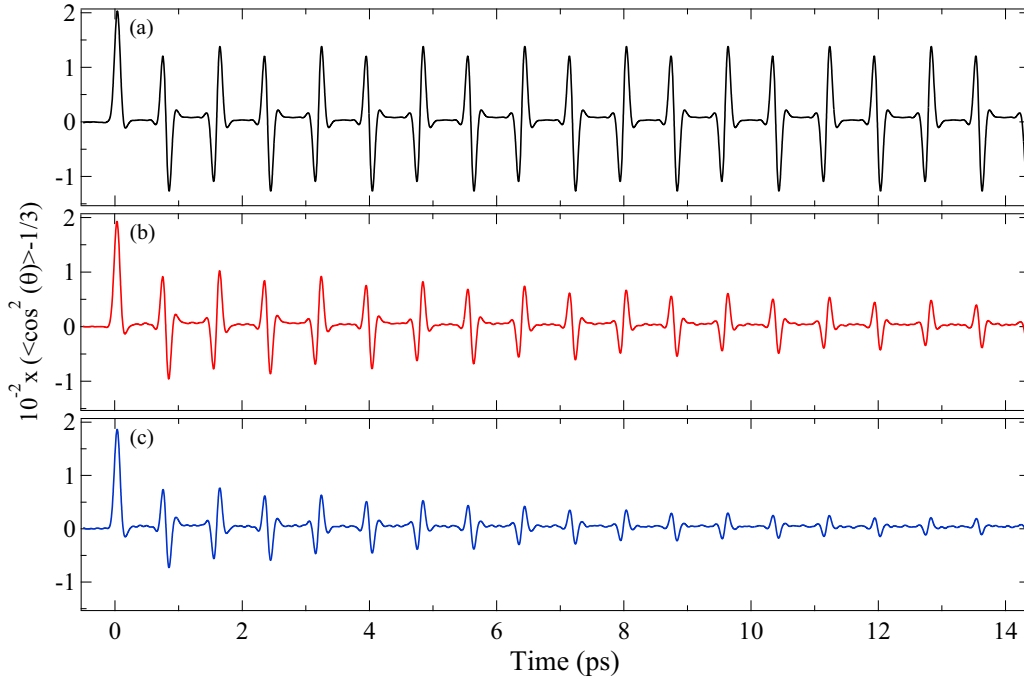


FIG. 5. rCMDS computed alignment traces for pure HCl at the densities of (a) 0.0, (b) 1.5, and (c) 3.0 amagat after excitation by a single laser pulse of peak intensity 20 TW/cm<sup>2</sup>.

$1/3(t)$ , which is the measured quantity, is straightforwardly derived.

As known since their discovery [24], alignment echoes following the excitation of gas molecules by two short laser pulses are a classical phenomenon, a characteristic demonstrated by the good agreement between purely classical simulations and measurements [18,34]. In contrast, this is not the case of the revivals generated by a single pulse, which result from the quantization and commensurability of the rotational speeds. Their modeling thus requires a requantization of the molecular rotation in the classical molecular dynamics simulations (rCMDS) for which the procedure proposed in [28] was applied. Since the equations of classical mechanics used in the rCMDS are exact, the quality of the associated predictions is only conditioned by the limits of the molecular-rotation requantization procedure and the quality of the input data, including the description of the laser pulse(s) and intermolecular potential. Concerning the first issue, it is difficult to quantify its influence but we expect it to be small, particularly for CO<sub>2</sub>, due to its small rotational constant. This statement is supported by previous comparisons between rCMDS predictions and absorption spectra showing that refined collisional effects are accurately predicted for both CO<sub>2</sub> [35,36] and HCl [15,37]. For the input data, tests show that the predicted decay rates are little sensitive to the laser pulse peak intensity and temporal shape, largely due to the nonadiabatic nature of the excitation. The influence of the intermolecular potential-energy surface is significant, with decay time constants that decrease as the strength of interactions increases. However, the PESs used have been obtained from accurate *ab initio* calculations and were successfully tested (see [22,23,30,31] and studies using them).

rCMDS were carried out for each of the considered systems at various densities, providing time dependencies of  $\langle \cos^2 \theta(t) - 1/3 \rangle$  which were treated, exactly as the experimental ones, to determine the decay time constants. The very good agreement between rCMDS-computed and measured traces around echoes was demonstrated in [34], and an agreement of similar quality is obtained for the HCl revivals, as shown by comparing Figs. 4 and 5. Note that the rCMDS enable one, in contrast with the measurements, to obtain the absolute value of the alignment factor (Fig. 5), demonstrating that the alignment efficiency is relatively weak, as could be expected from the small value of the HCl polarizability anisotropy [32]. Recall that rCMDS do take nonsecularity into account [18] and that they intrinsically include non-Markovian effects [see Figs. 2(a) and 2(b)]. However, they can mimic a Markovian behavior by disregarding all those molecules that are significantly interacting with a collision partner at the time of the (first) laser excitation. The efficiency of this trick is demonstrated for pure CO<sub>2</sub> by the comparison between Figs. 2(a) and 2(b) and Figs. 2(c) and 2(d). As well, secularity can be mimicked by progressively removing the contribution to the alignment factor of those molecules whose rotational speed has, since the end of the laser pulse, changed due to a collision.

## V. RESULTS AND DISCUSSION

The results of the experimentally and theoretically determined density-normalized decay time constants of the alignment features (echoes or revivals), reported in Fig. 6 for the studied systems of Table I, are discussed below.

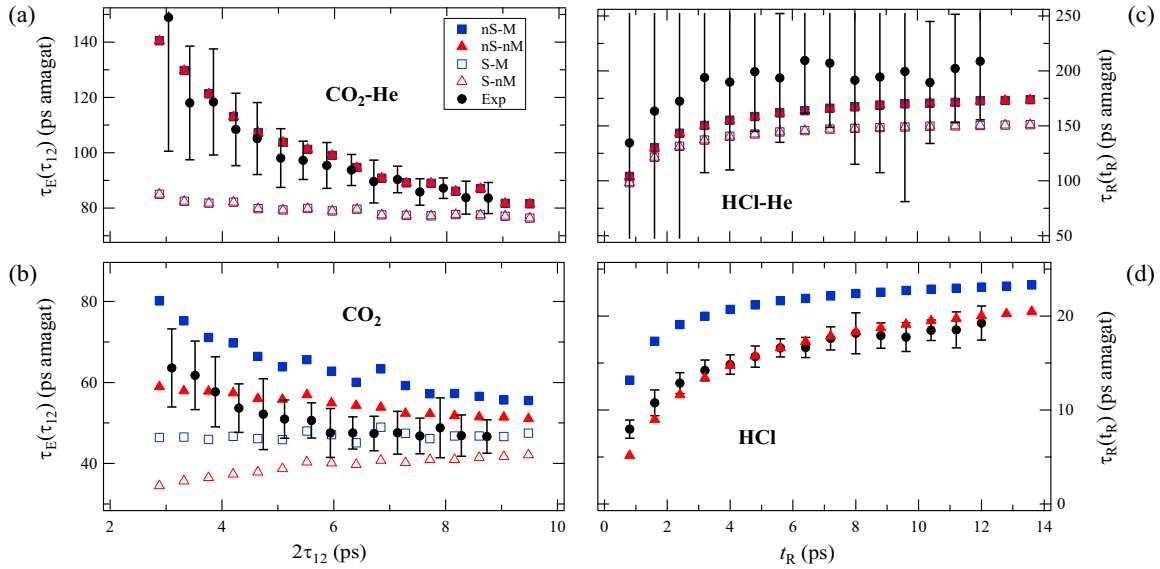


FIG. 6. Density-normalized time constants of the decays of alignment structures (echoes for  $\text{CO}_2$  and revivals for HCl) as functions of their time of appearance. The black full circles with error bars are values obtained from experiments, all other symbols having been deduced from rCMDS-computed alignment traces with a nonsecular and non-Markovian (nS-nM, red full triangles), a secular and non-Markovian (S-nM, red open triangles), a nonsecular and Markovian (nS-M, blue full squares), and a secular and Markovian (S-M, blue open squares) approach. Echoes for  $\text{CO}_2$  infinitely diluted in (a) He and (b) pure  $\text{CO}_2$ . Revivals for HCl infinitely diluted in (c) He and (d) pure HCl.

### A. $\text{CO}_2$ -He: a nonsecular but Markovian system

Recall that for  $\text{CO}_2$ -He collisions the Markov approximation is valid, so that the predictions obtained with and without this approximation are the same. As shown in Fig. 6(a), the secular assumption (open symbols) leads to inaccurate results over the entire time range studied, with errors that reduce as the delay increases. The associated rates are largely overestimated at the early stage of the dissipation process before agreement with experiment and nonsecular predictions is obtained at longer time delays, once the plateau region is reached (which is expected, from Sec. II, from visual extrapolation of the values in this plot, and from the results obtained for the very similar  $\text{N}_2\text{O}$ -He system [18], to be reached after a few tens of ps). In contrast, the nonsecular predictions do predict a large change of the pressure-induced decay of the echo amplitude, in very satisfactory agreement with the experimentally determined values. This confirms the importance of nonsecular effects for  $\text{CO}_2$  at early times expected from the preliminary analysis of Sec. II A and previous results [12] for the very similar  $\text{N}_2\text{O}$ -He system.

### B. $\text{CO}_2$ - $\text{CO}_2$ : a nonsecular and non-Markovian system

For pure  $\text{CO}_2$ , the results in Fig. 6(b) demonstrate that, among the values obtained with the various models, the non-Markovian and nonsecular predictions (full triangles) lead to the best agreement with the experimental results. In contrast, using either the Markovian or the secular approximation leads to significant discrepancies at short times before all predictions tend to become valid as the delay increases, all reaching the same plateau (which is expected, from Sec. II and from visual extrapolation of the results in this plot, to be reached after a few tens of ps). As for  $\text{CO}_2$ -He in Fig. 6(a), the

secular approach (open symbols) results, for pure  $\text{CO}_2$ , in an overestimation of the decay of early echoes with pressure, due to the disregarding of exchanges between some coherences which slow down the alignment dissipation at short times. Concerning the Markov approximation, its effect goes in the opposite direction (underestimation of the decay), because the significant and instantaneously efficient contribution of those collisions which are ongoing when the system experiences the first laser kick is neglected. These nonsecular and non-Markovian processes almost compensate each other in the case of pure  $\text{CO}_2$ , leading to full (nS-nM) predictions that only slightly depend on the delay, as do the experimental results.

### C. HCl-He: a secular and Markovian system

The results obtained from the revivals of HCl diluted in He are shown in Fig. 6(c). Note that the large error bars, when compared to those for  $\text{CO}_2$ -He,  $\text{CO}_2$  in Figs. 6(a) and 6(b) and for pure HCl in Fig. 6(d), come from the fact that the decay time constants for HCl(5%)-He(95%) are typically two times smaller than for HCl infinitely diluted in He, as explained in the Appendix. Although we believe that these uncertainties have been rigorously evaluated, they may be overestimated as indicated by the smooth evolution of the experimental mean values with  $t_R$ . Now recall that, for HCl-He, as for  $\text{CO}_2$ -He, the Markov approximation is valid, so that the results obtained with and without this approximation are the same. As can be seen, the experimental and theoretical results confirm the rapidly vanishing influence of nonsecular effects and quick reaching of the plateau expected from our preliminary analysis (Sec. II A).

#### D. HCl-HCl: a secular but non-Markovian system

The results obtained from the revivals of pure HCl are shown in Fig. 6(d). Since HCl shows small nonsecular effects at short times, as seen in Fig. 6(c), but is expected to show significant and long-lasting non-Markovian effects, due to the strong and long-range dipole-dipole interaction, only two computations were made, both nonsecular. The first (non Markovian) includes the contribution of collisions ongoing at  $t = 0$ , while the second (Markovian) disregards them. Figure 6(d) confirms the strong non-Markovianity, with effects at short times that considerably enhance the collisional dissipation rate (by a factor of nearly 3 for the first revival at  $t_R = 0.8$  ps with respect to the asymptotic value at long times according to the measurements, a change well predicted by the calculations). As the delay after the laser excitation increases, the decay time constant again tends toward a plateau (reached after a few tens of ps) and the Markov approximation progressively becomes valid.

### VI. TIME-DOMAIN VERSUS FREQUENCY-DOMAIN STUDIES

Line-mixing and finite-duration-of-collision effects, which are how the spectroscopic community respectively designates the influences of nonsecularity and non-Markovianity on pressure-broadened light-absorption and -scattering molecular spectra, have received significant attention in the past (see Chaps. IV and V in [9]). Recall that these spectra are obtained [9,13] from the Fourier transform of the autocorrelation function of the molecular dipole and polarizability, respectively, a transformation which enables one to switch from the time to the frequency domain as shown, for instance, in [38–40]. For a linear molecule, they thus involve the ensemble averages of  $\langle \cos \theta(t) \rangle$  and  $\langle \cos^2 \theta(t) \rangle$ , where  $\theta(t)$  is the change of the molecule axis direction since  $t = 0$ . The fact that these quantities have much in common with the alignment factor investigated in this paper enables us to point out that the findings of the present and frequency domain studies are similar, recalling that the characteristics of Fourier transformation imply that short times correspond to large frequency detunings and vice versa. Indeed, as widely demonstrated experimentally and theoretically (Chap. IV of [9]), disregarding line-mixing effects leads to the overestimation of the absorption (or scattering) of light in the wings of the optical resonances (see [41,42] for the CO<sub>2</sub>-He Markovian system also investigated in the present paper). *This is the direct equivalent of the underestimation of the decay time constant by the secular approach shown in Fig. 6(a).* Furthermore, investigating line- and band-wings regions for molecular pairs involving interactions at larger distances and lasting significantly longer than CO<sub>2</sub>-He has also enabled researchers to point out the breakdown of the impact (Markovian) approximation (see Chap. V in [9]). Predictions made disregarding the finite duration of collisions then underestimate the absorption in the line wings and the troughs between resonant transitions (see, e.g., [15] for the practically secular system HCl, and [14] for CO<sub>2</sub>). *This is the direct equivalent of the overestimation of the decay time constant by the Markovian model shown in Figs. 6(b) and 6(d).* Furthermore, it is worth noticing that the plateau

values at long delays, estimated from the experimental results in Figs. 6(a)–6(d) to be around 80 ps amagat for CO<sub>2</sub>-He, 200 ps amagat for HCl-He, 50 ps amagat for pure CO<sub>2</sub>, and 20 ps amagat for pure HCl, are very consistent with the corresponding pressure-broadening coefficient of absorption lines measured in the frequency domain. Indeed, the population-averaged values of these parameters are 83 ps amagat [43], 255 ps amagat [44], 51 ps amagat [45], and 23 ps amagat [46], respectively. This confirms the relation between this spectral parameter, which describes the collision-induced decay of the dipole autocorrelation function at long delays and is thus a secular and Markovian quantity, and the relaxation rate of alignment features at long delays.

Although there is a link between frequency and time domains, direct measurements of the system evolution at (very) short times, as done in the present paper, provide more valuable and detailed information than do those in the spectral domain for several reasons. The first is that the Fourier transform involved in the calculation of the spectrum “intricates” different times in the evolution of the relevant tensor (e.g., dipole) autocorrelation function. Although no information is lost, the way in which specific collisional effects manifest is somehow “fuzzier.” More importantly, pointing out nonsecular and/or non-Markovian effects in molecular spectra requires the availability of a predictive model that neglects them. This is generally achieved by computing the spectrum using purely Lorentzian line shapes [9], which requires *a priori* knowledge of many spectroscopic quantities including the positions, integrated intensities, and pressure-broadened widths of the various optical transitions. In contrast, the breakdown of the secular and/or Markov approximation may be directly detected, without use of any model, by experimentally studying the decay of alignment structures. Indeed, as shown in this paper, significant deviations between the collisional dissipation rates at short times and the asymptotic values at long delays [the plateau region where both approximations become valid, see Figs. 6(a)–6(d)] directly indicate their individual or simultaneous breakdown. Note that knowing if one (and then which one) or both of these approximations are involved requires some kind of model, but that semiquantitative indications can be brought by analyses (based on the rotational constant for the secular approximation and on the intermolecular potential and relative translational speed for the Markov approximation) such as those made in Secs. II A and II B. Last but not least, frequency-domain measurements require lasers of wavelengths properly adapted to the molecular system, or a spectrometer with a suitable spectral resolution if a broad light source is used. In contrast, the present paper based on molecular alignment relies on a nonresonant laser pulse excitation and therefore can be extended to any molecules provided they exhibit anisotropic polarizability, which only excludes spherical tops from the panel of investigatable systems.

### VII. CONCLUSION

By experimentally and theoretically studying the time dependence of the pressure-induced decay of alignment features induced in properly chosen gas molecules mixtures (HCl and CO<sub>2</sub>, pure and diluted in He) by intense and short laser pulse(s), we have probed the limits of the widely used secular

and Markov approximations. The measured and computed results obtained at very short delays (<15 ps) after the excitation show that non-Markovian (nonsecular) effects may considerably accelerate (slow down) the dissipation of the alignment at the early stage of the collision-induced decoherence process. This paper demonstrates, for linear rotors, that probing the evolution of the nonadiabatic laser-induced alignment very soon after the excitation directly provides (in contrast with spectral domain studies) detailed information on the roles played by nonsecularity and non-Markovianity in the collision-induced decoherence. Besides this “fundamental” interest, the fact that the short time delays correspond to large detunings from resonances in the frequency domain opens potential practical applications for planetary atmospheres science. Indeed, correct modeling of the associated line-wings regions (the so-called atmospheric transparency windows) where the absorption or emission of light is weak is essential for remote sensing of deep atmospheric layers as well as for radiative transfer and climate studies as discussed in Chap. VII of [9]. Our time-domain study thus appears as a complementary tool to test spectroscopic models taking line-mixing (i.e., nonsecular) and finite-duration-of-collision (i.e., non-Markovian) effects into account. These perspectives are further broadened by the fact that the approach tested here for prototype linear rotors can potentially be applied to molecules of more practical interest. These include nonlinear species, such as  $\text{NH}_3$ ,  $\text{H}_2\text{O}$ , and hydrocarbons, for instance, whose absorption spectra must be modeled beyond the secular and Markovian frames for studies of the atmospheres of various planets, as well as more exotic systems like molecules embedded or deposited in helium nanodroplets [47]. Finally, the approach used in this paper also appears as of interest to probe the influence of non-Markovianity on the short-time kinetics of reactive gas collisions, which opens the path toward chemistry and combustion studies.

#### ACKNOWLEDGMENTS

The work was supported by the Conseil Régional de Bourgogne Franche-Comté, EIPHI (Engineering and Innovation through Physical Sciences, High-technologies, and cross-disciplinary research) Graduate School (Grant No. ANR-17-EURE-0002) and has benefited from the facilities of the SMARTLIGHT platform in Bourgogne Franche-Comté (Grant No. ANR-21-ESRE-0040). J.M. acknowledges support from the China Scholarship Council. J.-M.H. benefited, for the computer simulations, from the IPSL mesocenter ESPRI (Ensemble of Services for Research at the IPSL) facility. J.W. acknowledges support by the National Key Research and Development Program (Grant No. 2018YFA0306303) and the National Natural Science Foundation of China (Grant No. 11834004). François Lique is thanked for discussing the HCl-He potential.

#### APPENDIX: PROTOCOL FOR MEASURING THE COLLISIONAL DECAY TIME CONSTANTS

A data series  $i$  is obtained by recording an alignment revival (for single pump pulse measurements) or an

echo (for two pump pulses experiments) produced around time  $t_n$  for different gas densities by varying the pressure in the static cell. For each time  $t_n$ , a nonlinear least-squares fitting procedure is applied in order to extract the single exponential decay time constant  $\tau_i(t_n)$  of the peak-to-dip amplitude of the revival (or echo) with an error bar  $\sigma_i(t_n)$  corresponding to two standard deviations. To reduce the latter, this exercise is repeated  $N$  times from which an averaged value  $\tau(t_n) = \sum_{i=1}^N W_i \tau_i(t_n) / \sum_{i=1}^N W_i$  and uncertainty  $\sigma(t_n) = (\sum_{i=1}^N W_i)^{-1/2}$  are calculated, with  $W_i = 1/\sigma_i^2(t_n)$ . This protocol is applied for a pure gas ( $\text{CO}_2$  or HCl), which enables one to estimate a time constant  $\tau_{100\%}(t_n) \pm \sigma_{100\%}(t_n)$ , and for a gas mixture, where the decay time constant  $\tau_{X\%}(t_n) \pm \sigma_{X\%}(t_n)$  of  $X\%$  of molecules ( $\text{CO}_2$  or HCl) diluted in  $(100 - X)\%$  of He is calculated. The collisional decay times  $\tau_{0\%}$  corresponding to molecules infinitely diluted in He is calculated by assuming binary collisions (justified in present conditions) using the relation  $\frac{1}{\tau_{X\%}} = \frac{C_{\text{Mol}}}{\tau_{100\%}} + \frac{C_{\text{He}}}{\tau_{0\%}}$ , where  $C_{\text{Mol}} = X/100$  and  $C_{\text{He}} = 1 - X/100$  are the concentration of molecules and He atoms, respectively. The uncertainty within two standard deviations of this quantity is obtained by the following equation:

$$\sigma_{0\%} = \sqrt{\frac{\tau_{0\%}^4}{\tau_{X\%}^4} \frac{\sigma_{X\%}^2}{C_{\text{He}}^2} + \frac{C_{\text{Mol}}^2}{C_{\text{He}}^2} \frac{\tau_{0\%}^4}{\tau_{100\%}^4} \sigma_{100\%}^2}. \quad (\text{A1})$$

Note that for high dilutions ( $C_{\text{Mol}}/C_{\text{He}} \ll 1$ , i.e.,  $C_{\text{He}} \simeq 1$ ) the last quantity can be approximated by

$$\sigma_{0\%} \approx \frac{\tau_{0\%}^2}{\tau_{X\%}^2} \sigma_{X\%}. \quad (\text{A2})$$

Equation (A2) shows that, first, the uncertainty for the infinitely diluted value is, for (HCl,  $\text{CO}_2$ )-He, always larger than that of the (95% He) mixture since one always has  $\tau_{100\%} \leq \tau_{0\%}$  [compare Fig. 6(a) with Fig. 6(b), and Fig. 6(c) with Fig. 6(d)] thus leading to  $\tau_{X\%} \leq \tau_{0\%}$  and, second, its amplitude scales with the square of the ratio  $\tau_{0\%}/\tau_{X\%}$ . In the case of  $\text{CO}_2$ -He, this ratio is close to unity, whereas for HCl-He, its maximum value is about 2, which explains the much larger uncertainties on the time constant of HCl-He as compared to  $\text{CO}_2$ -He. Note that this is further emphasized by the second term below the square root in Eq. (A1) which is also significantly larger in the case of HCl than for  $\text{CO}_2$ .

In order to reduce error bars, alignment revivals (HCl and HCl-He) have been recorded for up to ten total pressures and, in the case of the echoes ( $\text{CO}_2$  and  $\text{CO}_2$ -He), 15 delays between the two pump pulses. Altogether, the experimental values displayed in Fig. 6 are the results of about 2600 specific alignment signal recordings.

- [1] H.-P. Breuer, E.-M. Laine, J. Piilo, and B. Vacchini, Colloquium: Non-Markovian dynamics in open quantum systems, *Rev. Mod. Phys.* **88**, 021002 (2016).
- [2] I. de Vega and D. Alonso, Dynamics of non-Markovian open quantum systems, *Rev. Mod. Phys.* **89**, 015001 (2017).
- [3] L. Li, M. J. W. Hall, and H. M. Wiseman, Concepts of quantum non-Markovianity: A hierarchy, *Phys. Rep.* **759**, 1 (2018).
- [4] C. P. Koch, M. Lemesko, and D. Sugny, Quantum control of molecular rotation, *Rev. Mod. Phys.* **91**, 035005 (2019).
- [5] M. O. Scully, K. R. Chapin, K. E. Dorfman, M. B. Kim, and A. Svidzinsky, Quantum heat engine power can be increased by noise-induced coherence, *Proc. Natl. Acad. Sci. USA* **108**, 15097 (2011).
- [6] C. Monroe, Quantum information processing with atoms and photons, *Nature (London)* **416**, 238 (2002).
- [7] R. W. Schoenlein, L. A. Peteanu, R. A. Mathies, and C. V. Shank, The first step in vision: Femtosecond isomerization of rhodopsin, *Science* **254**, 412 (1991).
- [8] G. S. Engel, T. R. Calhoun, E. L. Read, T.-K. Ahn, T. Mančal, Y.-C. Cheng, R. E. Blankenship, and G. R. Fleming, Evidence for wavelike energy transfer through quantum coherence in photosynthetic systems, *Nature (London)* **446**, 782 (2007).
- [9] J.-M. Hartmann, C. Boulet, and D. Robert, *Collisional Effects on Molecular Spectra. Laboratory Experiments and Models, Consequences for Applications*, 2nd ed. (Elsevier, Amsterdam, 2020).
- [10] J. O. Hirschfelder, C. F. Curtiss, and R. B. Bird, *Molecular Theory of Gases and Liquids*, 2nd ed. (Wiley, New York, 1964).
- [11] V. May and O. Kuhn, *Charge and Energy Transfer Dynamics in Molecular Systems* (Wiley, New York, 2011).
- [12] J. Ma, H. Zhang, B. Lavorel, F. Billard, E. Hertz, J. Wu, C. Boulet, J.-M. Hartmann, and O. Faucher, Observing collisions beyond the secular approximation limit, *Nat. Commun.* **10**, 5780 (2019).
- [13] P. Rayer, *Pressure Broadening of Spectral Lines* (Cambridge University, Cambridge, England, 2020).
- [14] L. Ozanne, Q. Ma, Nguyen-Van-Thanh, C. Brodbeck, J. P. Bouanich, J. M. Hartmann, C. Boulet, and R. H. Tipping, Line-mixing, finite duration of collision, vibrational shift, and non-linear density effects in the  $\nu_3$  and  $3\nu_3$  bands of  $\text{CO}_2$  perturbed by Ar up to 1000 bar, *J. Quant. Spectrosc. Radiat. Transfer* **58**, 261 (1997).
- [15] H. Tran, G. Li, V. Ebert, and J.-M. Hartmann, Super- and sub-Lorentzian effects in the Ar-broadened line wings of HCl gas, *J. Chem. Phys.* **146**, 194305 (2017).
- [16] H. Stapelfeldt and T. Seideman, Colloquium: Aligning molecules with strong laser pulses, *Rev. Mod. Phys.* **75**, 543 (2003).
- [17] S. Ramakrishna and T. Seideman, Intense Laser Alignment in Dissipative Media as a Route to Solvent Dynamics, *Phys. Rev. Lett.* **95**, 113001 (2005).
- [18] J. M. Hartmann, J. Ma, T. Delahaye, F. Billard, E. Hertz, J. Wu, B. Lavorel, C. Boulet, and O. Faucher, Molecular alignment echoes probing collision-induced rotational-speed changes, *Phys. Rev. Res.* **2**, 023247 (2020).
- [19] P. M. Felker, J. S. Baskin, and A. H. Zewail, Rephasing of collisionless molecular rotational coherence in large molecules, *J. Phys. Chem.* **90**, 724 (1986).
- [20] J. Ortigoso, M. Rodriguez, M. Gupta, and B. Friedrich, Time evolution of pendular states created by the interaction of molecular polarizability with a pulsed nonresonant laser field, *J. Chem. Phys.* **110**, 3870 (1999).
- [21] F. Haake and M. Lewenstein, Adiabatic drag and initial slip in random processes, *Phys. Rev. A* **28**, 3606 (1983).
- [22] T. Korona, R. Moszynski, F. Thibault, J.-M. Launay, B. Bussery-Honvault, J. Boissoles, and P. E. S. Wormer, Spectroscopic, collisional, and thermodynamic properties of the He- $\text{CO}_2$  complex from an *ab initio* potential: Theoretical predictions and confrontation with the experimental data, *J. Chem. Phys.* **115**, 3074 (2001).
- [23] S. Bock, E. Bich, and E. Vogel, A new intermolecular potential energy surface for carbon dioxide from *ab initio* calculations, *Chem. Phys.* **257**, 147 (2000).
- [24] G. Karras, E. Hertz, F. Billard, B. Lavorel, J. M. Hartmann, O. Faucher, E. Gershnel, Y. Prior, and I. S. Averbukh, Orientation and Alignment Echoes, *Phys. Rev. Lett.* **114**, 153601 (2015).
- [25] K. Lin, P. Lu, J. Ma, X. Gong, Q. Song, Q. Ji, W. Zhang, H. Zeng, J. Wu, G. Karras, G. Siour, J.-M. Hartmann, O. Faucher, E. Gershnel, Y. Prior, and I. S. Averbukh, Echoes in Space and Time, *Phys. Rev. X* **6**, 041056 (2016).
- [26] D. Rosenberg, R. Damari, and S. Fleischer, Echo Spectroscopy in Multilevel Quantum-Mechanical Rotors, *Phys. Rev. Lett.* **121**, 234101 (2018).
- [27] B. Lavorel, P. Babilotte, G. Karras, F. Billard, E. Hertz, and O. Faucher, Measurement of dichroism in aligned molecules, *Phys. Rev. A* **94**, 043422 (2016).
- [28] J. M. Hartmann and C. Boulet, Quantum and classical approaches for rotational relaxation and nonresonant laser alignment of linear molecules: A comparison for  $\text{CO}_2$  gas in the nonadiabatic regime, *J. Chem. Phys.* **136**, 184302 (2012).
- [29] M. P. Allen and D. J. Tildesley, *Computer Simulation of Liquids* (Clarendon, Oxford, 1987).
- [30] Y. Ajili, K. Hammami, N. E. Jaidane, M. Lanza, Y. N. Kalugina, F. Lique, and M. Hochlaf, On the accuracy of explicitly correlated methods to generate potential energy surfaces for scattering calculations and clustering: Application to the HCl-He complex, *Phys. Chem. Chem. Phys.* **15**, 10062 (2013).
- [31] P. K. Naicker, A. K. Sum, and S. I. Sandler, *Ab initio* pair potential and phase equilibria predictions for hydrogen chloride, *J. Chem. Phys.* **118**, 4086 (2003).
- [32] G. Maroulis, A systematic study of basis set, electron correlation, and geometry effects on the electric multipole moments, polarizability, and hyperpolarizability of HCl, *J. Chem. Phys.* **108**, 5432 (1998).
- [33] A. P. Kouzov and M. Chrysos, Collision-induced absorption by  $\text{CO}_2$  in the far infrared: Analysis of leading-order moments and interpretation of the experiment, *Phys. Rev. A* **80**, 042703 (2009).
- [34] H. Zhang, B. Lavorel, F. Billard, J. M. Hartmann, E. Hertz, O. Faucher, J. Ma, J. Wu, E. Gershnel, Y. Prior, and I. S. Averbukh, Rotational Echoes as a Tool for Investigating Ultrafast Collisional Dynamics of Molecules, *Phys. Rev. Lett.* **122**, 193401 (2019).
- [35] J.-M. Hartmann and C. Boulet, Molecular dynamics simulations for  $\text{CO}_2$  spectra. III. Permanent and collision-induced tensors contributions to light absorption and scattering, *J. Chem. Phys.* **134**, 184312 (2011).

- [36] H. T. Nguyen, N. H. Ngo, and H. Tran, Prediction of line shape parameters and their temperature dependences for  $\text{CO}_2\text{-N}_2$  using molecular dynamics simulations, *J. Chem. Phys.* **149**, 224301 (2018).
- [37] H. Tran and J.-L. Domenech, Spectral shapes of Ar-broadened HCl lines in the fundamental band by classical molecular dynamics simulations and comparison with experiments, *J. Chem. Phys.* **141**, 064313 (2014).
- [38] S. Kinoshita, Y. Kai, M. Yamaguchi, and T. Yagi, Direct comparison of femtosecond fourier-transform Raman spectrum with spontaneous light scattering spectrum, *Chem. Phys. Lett.* **236**, 259 (1995).
- [39] A. Rouz , V. Boudon, B. Lavorel, O. Faucher, and W. Raballand, Rotational Raman spectroscopy of ethylene using a femtosecond time-resolved pump-probe technique, *J. Chem. Phys.* **123**, 154309 (2005).
- [40] H. Zhang, F. Billard, O. Faucher, and B. Lavorel, Time-domain measurement of pure rotational Raman collisional linewidths of ethane  $\text{C}_2\text{H}_6$ , *J. Raman Spectrosc.* **49**, 1350 (2018).
- [41] L. Ozanne, N. Van Thanh, C. Brodbeck, J. P. Bouanich, J. M. Hartmann, and C. Boulet, Line mixing and nonlinear density effects in the  $\nu_3$  and  $3\nu_3$  infrared bands of  $\text{CO}_2$  perturbed by He up to 1000 bar, *J. Chem. Phys.* **102**, 7306 (1995).
- [42] N. N. Filippov and M. V. Tonkov, Semiclassical analysis of line mixing in the infrared bands of CO and  $\text{CO}_2$ , *J. Quant. Spectrosc. Radiat. Transfer* **50**, 111 (1993).
- [43] F. Thibault, J. Boissoles, R. Le Doucen, J. P. Bouanich, P. Arcas, and C. Boulet, Pressure induced shifts of  $\text{CO}_2$  lines: Measurements in the  $00^0_3\text{-}00^0_0$  band and theoretical analysis, *J. Chem. Phys.* **96**, 4945 (1992).
- [44] G. Li, R. E. Asfin, A. V. Domanskaya, and V. Ebert, He-broadening and shifting coefficients of HCl lines in the  $(1 \leftarrow 0)$  and  $(2 \leftarrow 0)$  infrared transitions, *Mol. Phys.* **116**, 3495 (2018).
- [45] A. Predoi-Cross, A. V. Unni, W. Liu, I. Schofield, C. Holladay, A. R. W. McKellar, and D. Hurtmans, Line shape parameters measurement and computations for self-broadened carbon dioxide transitions in the  $30012 \leftarrow 00001$  and  $30013 \leftarrow 00001$  bands, line mixing, and speed dependence, *J. Mol. Spectrosc.* **245**, 34 (2007).
- [46] A. S. Pine and A. Fried, Self-broadening in the fundamental bands of HF and HCl, *J. Mol. Spectrosc.* **114**, 148 (1985).
- [47] H. H. Kristensen, L. Kranabetter, C. A. Schouder, C. Stapper, J. Arlt, M. Mudrich, and H. Stapelfeldt, Quantum-State-Sensitive Detection of Alkali Dimers on Helium Nanodroplets by Laser-Induced Coulomb Explosion, *Phys. Rev. Lett.* **128**, 093201 (2022).